Shedding light on thermal photon and dilepton production

Greg Jackson[1,*]

[1]Institute for Nuclear Theory, Box 351550, University of Washington, Seattle, WA 98195-1550, United States

Abstract. Electromagnetic radiation from the quark-gluon plasma (QGP) is an important observable to be considered in heavy ion collision experiments. I will provide an update on recent advancements from perturbation theory and quenched lattice simulations. The resummed next-to-leading order (NLO) emission rate has recently been decomposed into transverse and longitudinal components, and extended to non-zero baryon chemical potential. The associated spectral function has also been tested against the Euclidean correlator, for continuum-extrapolated lattice data (at $\mu_{\rm B} = 0$).

1 Introduction

Quarks undergoing acceleration in the deconfined state of QCD matter can generate electromagnetic radiation, with those photons that are off-shell subsequently decaying into lepton-antilepton pairs. Therefore, both the real photon spectrum and dilepton invariant mass distribution can provide access to properties of the hot quark-gluon plasma (QGP) that exists in heavy ion collision experiments [1–3]. In this report, I will show that the spectral function can be constrained by lattice data and discuss how the presence of a baryon chemical potential, $\mu_{\rm B}$, impacts the production of photons and dileptons. While the latter has been examined for real photons [4], we present new results away from the light cone. This involves properly understanding how $\mu_{\rm B}$ enters the strict NLO computation, the so-called LPM effect (at low invariant masses), and how to smoothly interpolate between the two regimes as originally advocated in ref. [5].

To start, we fix the notation and denote the temperature by T , the quark chemical potential by μ and the energy and momentum with respect to the plasma rest frame of the lepton pair by ω and $\boldsymbol{k}$ respectively. In chemical equilibrium, $\mu = \frac{1}{3}\mu_{\rm B}$ and thermal averages are calculated from $\langle ... \rangle = {\rm Tr}[\,\hat{\varrho}\,(...)\,]$ with the density matrix $\hat{\varrho} = \mathcal{Z}^{-1} e^{-(\hat{H}-\mu\hat{Q})/T}$ [6]. Emission rates can then be derived from an associated spectral function. In this case, the relevant spectral function is given by the imaginary part of the current-current correlation function, evaluated at the energy $k_0 = \omega + i0^+$, namely

$$\rho_{\mu\nu}(\omega, \boldsymbol{k}) = {\rm Im}\left[\Pi_{\mu\nu}(K)\right], \tag{1}$$

where $K = (k_0, \boldsymbol{k})$ and the correlation function being given by[1]

$$\Pi_{\mu\nu}(K) \;\equiv\; -\int_0^{1/T} {\rm d}\tau \int_{\boldsymbol{x}} e^{k_0\tau + i\,\boldsymbol{k}\cdot\boldsymbol{x}} \left\langle J_\mu(t,\boldsymbol{x})\, J_\nu(0,\boldsymbol{0}) \right\rangle, \quad J_\mu \equiv \bar{\psi}\gamma_\mu\psi\ . \tag{2}$$

*e-mail: gsj6@uw.edu

[1]An overall minus sign appears in (2) for sake of convenience.

The thermal average is taken on a volume with periodic temporal extent $\tau \in (0, T^{-1})$ and k_0 is a bosonic Matsubara frequency $k_0 = i\,2\pi z T$ with $z \in \mathbb{Z}$.

With these definitions, the differential photon rate involves the spectral function $\rho_{\rm V} \equiv \rho_\mu^{\ \mu}$ for both *i*) real and *ii*) virtual photons. In case *i*), $\omega = |\boldsymbol{k}| \equiv k$ and case *ii*) provides the dilepton rate with the invariant mass $M \equiv \sqrt{K^2}$ that should be above the threshold to form the pair: $K^2 = \omega^2 - k^2 > 4m_\ell^2$. One might also consider *iii*) deep inelastic scattering on a QGP target, which would involve $\rho_{\rm V}$ for timelike virtualities [7]. Although case *iii*) may not be experimentally accessible, there is another good reason to pursue $K^2 < 0$: Knowing the spectral function at fixed k for *all* ω, enables one to calculate the imaginary time correlation function and thus connect with non-perturbative lattice measurements (at $\mu = 0$).

The gross features of $\rho_{\rm V}$ can be understood from the leading-order (LO) process $q\bar{q} \to \gamma^\star$, i.e. $\alpha_s = 0$. For non-zero μ, the result was determined in ref. [8] for $K^2 > 0$. In general, for any ω, the free spectral function is given by the strict 1-loop result[2]

$$\rho_{\rm V}\big|^{\rm strict}_{\rm 1-loop} \;=\; \frac{N_{\rm c}K^2}{4\pi}\Big\{\sum_{\nu=\pm\mu}\frac{T}{k}\ln\Big[\frac{1+e^{\nu-\frac{1}{2}(\omega+k)/T}}{1+e^{\nu-\frac{1}{2}|\omega-k|/T}}\Big] + \Theta(K^2)\Big\}\,, \tag{3}$$

where Θ denotes the Heaviside step function and $N_{\rm c}$ is the number of colours. This is depicted in fig. 1, assuming non-zero T. The vanishing of $\rho_{\rm V}$ for $\omega = k$ is readily understood from kinematics and the μ-dependence stems from the relative enhancement and depletion of quarks and antiquarks respectively (for $\mu > 0$).

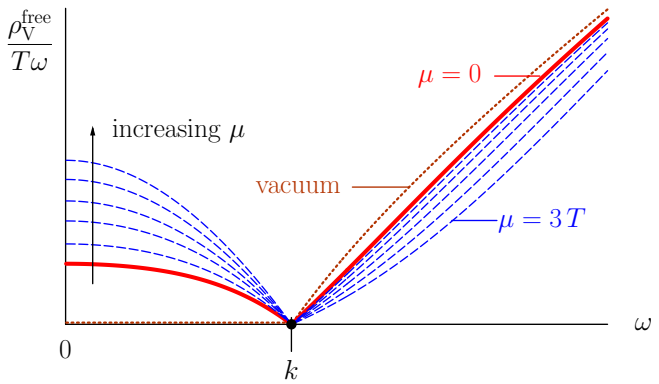

Figure 1. Sketch of the free spectral function ($\alpha_s = 0$), with the $\mu = 0$ result (solid) and the impact of $\mu > 0$ also shown (dashed). The limit $T, \mu \to 0$ of eq. (3) is the vacuum result (dotted).

2 Weak coupling QCD corrections

Corrections to (3) may be computed in perturbation theory, however the structure of the expansion in α_s depends on the (parametric) value of K^2. Away from the light cone, $|K^2| \gtrsim (\pi T)^2$, the 2-loop corrections may be calculated directly and the NLO terms are $O(\alpha_s)$ [10]. However, for small K^2 as the free result (3) gets kinematically suppressed (and, in particular vanishes for $K^2 = 0$) implying that the QCD 'corrections' actually represent the first non-trivial approximation to the real photon rate. For $K^2 \lesssim (gT)^2$ certain diagrams need to be

[2] Setting $\mu = 0$ gives eq. (2.4) from ref. [9].

resummed to obtain a meaningful result, which is motivated on physics grounds to describe thermal screening [11–13] in addition to the Landau-Pomeranchuk-Migdal (LPM) effect [14–17]. These contributions alter the asymptotic dependence on the strong coupling α_s to a leading-logarithm $\rho_{\rm V} \sim \alpha_s \ln(1/\alpha_s) T^2$ as $\alpha_s \to 0$.

In ref. [5], a simple procedure to interpolate between these two regimes was proposed. Care is required to avoid double counting when resummation is combined with the strict NLO expansion. A full resummed spectral functions can be defined as

$$\rho_{\rm V}|^{\rm resummed}_{\rm NLO} \;\equiv\; \rho_{\rm V}|^{\rm strict}_{\rm 1-loop} + \rho_{\rm V}|^{\rm strict}_{\rm 2-loop} + \big(\rho_{\rm V}|^{\rm full}_{\rm LPM} - \rho_{\rm V}|^{\rm expanded}_{\rm LPM}\big)\,, \tag{4}$$

where the subtracted term in parenthesis represent the 1- and 2-loop parts that are included in the full LPM result (with certain approximations). For (4) to make sense, a delicate cancellation must take place around $\omega \simeq k$ so that the result is finite and continuous there [9]. The details of the LPM 'full' and 'expanded' will be provided in sec. 5, where we focus on non-zero baryon density.

In ref. [18], we studied (with full generality) the types of interactions that would contribute to strict NLO rates and developed a numerical routine for *any* combination of particles, masses, chemical potentials and a wide class of matrix elements. For the dilepton rate, it is preferable to use a more tailored approach which requires a 2-dimensional phase space integration [19]. The underlying spectral function can be reduced to a set of elementary 'master integrals' at NLO (some of which were studied for $\omega > k$ in [10]), which are uniformly defined by

$$\rho^{(m,n)}_{abcde}(K) \;\equiv\; {\rm Im} \sum\!\!\!\!\!\!\int_{P,Q} \frac{p_0^m\, q_0^n}{[P^2]^a\,[Q^2]^b\,[R^2]^c\,[L^2]^d\,[V^2]^e}\bigg|_{R=K-P-Q\,,\;L=K-P\,,\;V=K-Q}\,. \tag{5}$$

Functions of this kind provide a basis onto which the general 2-loop topology (after carrying out the Dirac algebra, etc.) can be mapped for self energies with external momentum K. In the sum-integrals (5),[3] P and Q are fermionic momenta with $p_0 = i(2x+1)\pi T + \mu$ and $q_0 = i(2y+1)\pi T - \mu$ (where $x, y \in \mathbb{Z}$). (Recall that K is bosonic, thus $R = K - P - Q$ is also bosonic while $L = K - P$ and $V = K - Q$ are fermionic.)

3 Non-perturbative constraints

Although real-time rates are difficult to compute from numerical Monte Carlo simulations, the τ dependence of the integrand in eq. (2) can be obtained from Euclidean lattices. The imaginary-time correlation function $G_{\mu\nu}(\tau, k)$ is related to the spectral function from (1) via the integral transform[4]

$$\begin{aligned} G_{\mu\nu}(\tau,k) \;=\; \int_0^\infty \frac{{\rm d}\omega}{2\pi} \;\Big\{\; & \Big(\rho_{\mu\nu}(\omega,k) - \rho_{\mu\nu}(-\omega,k)\Big)\frac{\cosh\big[\omega(\frac{1}{2T}-\tau)\big]}{\sinh[\frac{1}{2T}\omega]} \\ & + \Big(\rho_{\mu\nu}(\omega,k) + \rho_{\mu\nu}(-\omega,k)\Big)\frac{\sinh\big[\omega(\frac{1}{2T}-\tau)\big]}{\sinh[\frac{1}{2T}\omega]} \;\Big\}\,. \end{aligned} \tag{6}$$

[3] To be crystal clear, the sum-integrals are (in $4-2\epsilon$ spacetime dimensions)

$$\sum\!\!\!\!\!\!\int_P = \int_{\boldsymbol{p}} T\sum_{p_0}\,, \qquad \int_{\boldsymbol{p}} = \Big(\frac{e^\gamma \bar{\mu}^2}{4\pi}\Big)^\epsilon \int \frac{d^d p}{(2\pi)^d}\,.$$

[4] In practice, all the spectral functions studied here are antisymmetric in $\omega \to -\omega$ and therefore only the first term on the right hand side of eq. (6) contributes.

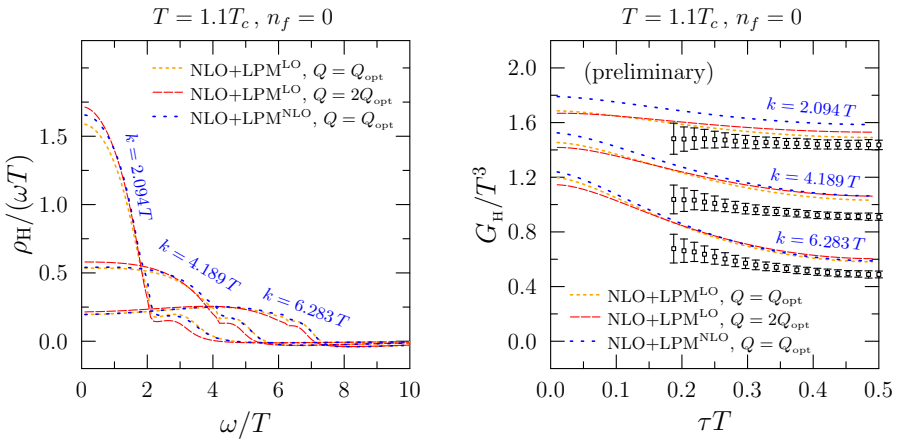

Figure 2. Results for $\rho_{\rm H}$ (left) and the corresponding Euclidean correlation function, calculated from eq. (6), (right) at $T = 1.1T_c$ for $n_f = 0$. Similar plots for $\rho_{\rm V}$ (and $G_{\rm V}$) may be found in ref. [9].

It is a formidable task to invert (6) and thus obtain the spectral function directly from a finite set of sampling points [20, 21].

Rather than using (6) to obtain $\rho_{\rm V}$ (from $G_{\rm V}$), another spectral function turns out to be convenient:

$$\rho_{\rm H} \quad \equiv \quad \rho_{\rm V} + 3\frac{K^2}{k^2}\rho_{00}\,, \tag{7}$$

which is highly suppressed in the ultraviolet and exactly vanishes in vacuum. This makes the corresponding Euclidean correlator more sensitive to the infrared physics of interest [22]. We point out that $\rho_{\rm V}$ and $\rho_{\rm H}$ agree on the light cone, but differ considerably for $\omega \neq k$. The spectral function (7) satisfies a sum rule, $\int_0^\infty {\rm d}\omega\,\omega\,\rho_{\rm H}(\omega,k) = 0$, which supplies additional restrictions on any inversion candidates. Computing both $\rho_{\rm V}$ and $\rho_{\rm H}$ amounts to determining separately the transverse and longitudinal components, thus specifying the entire tensor $\rho_{\mu\nu}$.

One may also use (6) to compute $G_{\mu\nu}$ from models of the spectral function. In fig. 2 the perturbative results for $\rho_{\rm H}$ and $G_{\rm H}$ are shown, compared with continuum extrapolated lattice data for quenched QCD from ref. [23]. The various curves show different choices of the scale in the running coupling, Q, as well as including the NLO part of the LPM computation [24]. (Further details may be found in refs. [9, 25].)

4 Beyond leading-order: strict NLO

The strict NLO result for $\rho_{\rm V}$ can be expressed as a linear combination of the master integrals, defined by eq. (5). Evaluating the diagrams, we obtain the result

$$\begin{aligned}
\rho_{\rm V}|^{(g^2)}_{\rm NLO} \quad &= \qquad\qquad\qquad\qquad\qquad\qquad\qquad\qquad\qquad\qquad\qquad\qquad (8)\\
8(1-\epsilon)g^2C_{\rm F}N_{\rm c}\;\Big\{\;&(1-\epsilon)K^2\Big(\rho^{(0,0)}_{11020}+\rho^{(0,0)}_{11002}-\rho^{(0,0)}_{10120}-\rho^{(0,0)}_{01102}\Big)+\rho^{(0,0)}_{11010}+\rho^{(0,0)}_{11001}\\
&+\;\;2\epsilon\,\rho^{(0,0)}_{11100}\;+\;2\frac{K^2}{k^2}\rho^{(1,1)}_{11011}\;-\;\tfrac{1}{2}K^2\Big(\frac{\omega^2}{k^2}+3+2\epsilon\Big)\rho^{(0,0)}_{11011}\\
&-\;\;(1-\epsilon)\Big(\rho^{(0,0)}_{1111(-1)}+\rho^{(0,0)}_{111(-1)1}\Big)+2K^2\Big(\rho^{(0,0)}_{11110}+\rho^{(0,0)}_{11101}\Big)-K^4\rho^{(0,0)}_{11111}\;\Big\}\,,
\end{aligned}$$

where $C_{\rm F} = (N_{\rm c}^2 - 1)/(2N_{\rm c})$. Above, the limit $\epsilon \to 0$ is implied because some of the master integrals have $1/\epsilon$-contributions stemming from their vacuum parts. Note that the spectral function is symmetric in the simultaneous exchanges: $a \leftrightarrow b$, $d \leftrightarrow e$ and $m \leftrightarrow n$ for the master integrals. Consequently, the result will be unchanged by $\mu \to -\mu$. In the case where $\mu = 0$, the additional symmetry $\rho^{(m,n)}_{abcde} \to \rho^{(n,m)}_{baced}$ leads to the same decomposition as in ref. [9, 19].

An important cross-check of the result (8) (besides the obvious, gauge invariance etc.) can be found within the *hard thermal loop* (HTL) approximation, for which the master integrals can be computed in closed form. The HTL limit is given by the small-K behaviour of $\Pi_{\mu\nu}$ and the 1-loop result is well known [6]. Recently, the 2-loop HTL photon self energy was computed for a hot and dense QED plasma in ref. [26]. We restate the outcome here, in a way that is compatible with eq. (2),

$$\Pi_{\rm V}^{\rm HTL} \;=\; -\Big(\tfrac{1}{3}T^2 + \frac{\mu^2}{\pi^2}\Big) + \frac{e^2}{8\pi^2}\Big(T^2 + \frac{\mu^2}{\pi^2}\Big)\Big(1 + \frac{\omega}{k}L\Big) + \frac{e^2}{4\pi^2}\,\frac{\mu^2}{\pi^2}\Big(1 - \frac{\omega^2}{k^2}\Big)\Big(1 - \frac{\omega}{2k}L\Big)^2 , \tag{9}$$

where $L = \ln\frac{\omega+k+i0^+}{\omega-k+i0^+}$. This result can be transcribed to the present case by replacing $e^2 \to g^2 C_{\rm F} N_{\rm c}$ in eq. (9), so that the resulting spectral function should coincide with the strict NLO version of $\rho_{\rm V}$ (8) assuming ω and k are small. The agreement between the two approaches has been verified both analytically and numerically. Worth mentioning explicitly, is the HTL limit for the $\rho^{(1,1)}_{11011}$ master integral.[5] One may readily check that

$$\sum\!\!\!\!\!\!\int_{P,Q} \frac{p_0 q_0}{P^2 Q^2 (K-P)^2 (K-Q)^2} \;\approx\; -\frac{\mu^2}{4(2\pi)^4}\Big(1 - \frac{\omega}{2k}L\Big)^2 . \tag{10}$$

This term appears when the strict 2-loop self energy, $\Pi_{\rm V}|^{(g^2)}_{\rm NLO}$, is evaluated and is entirely responsible for the last term in (9), which contains a new structure involving a squared logarithm (only present at finite density).

5 Beyond leading-order: LPM regime

The master integrals $\rho^{(0,0)}_{1111(-1)}$ and $\rho^{(0,0)}_{111(-1)1}$ from eq. (8) each contain a log-divergence as $K^2 \to 0^{\pm}$ [25]. This is a signal that resummation is required, and the LPM framework serves that purpose. Two important scales enter in the problem: The Debye mass m_D and the asymptotic quark mass m_∞, both of which are modified by the chemical potential, *viz.*

$$m_D^2 \;\equiv\; g^2\Big[\Big(\tfrac{1}{2}n_f + N_{\rm c}\Big)\frac{T^2}{3} + n_f\,\frac{\mu^2}{2\pi^2}\Big], \qquad m_\infty^2 \;\equiv\; g^2\,\frac{C_{\rm F}}{4}\Big(T^2 + \frac{\mu^2}{\pi^2}\Big), \tag{11}$$

where n_f is the number of light quark flavours. Following ref. [15] in impact parameter space, the result can be expressed as[6]

$$\begin{aligned}\rho_{\rm V}|^{\rm full}_{\rm LPM} \;&=\; -\frac{N_{\rm c}}{\pi}\int_{-\infty}^{\infty}\!{\rm d}p\,\big[1 - n_{\rm F}(p-\mu) - n_{\rm F}(\omega - p + \mu)\big] \\ &\times\; \lim_{\boldsymbol{b}\to\boldsymbol{0}}\,\mathbb{P}\Big\{\frac{K^2}{\omega^2}\,{\rm Im}[g(\boldsymbol{b})] + \frac{1}{2}\Big[\frac{1}{p^2} + \frac{1}{(\omega-p)^2}\Big]\,{\rm Im}[\nabla_\perp \cdot \boldsymbol{f}(\boldsymbol{b})]\Big\}\,,\end{aligned} \tag{12}$$

[5] If $\mu = 0$, one can prove that $\rho^{(1,1)}_{11011} = \frac{1}{4}\omega^2\rho^{(0,0)}_{11011}$ which vanishes in the HTL approximation when ω is soft.
[6] A formulation with better asymptotics (for large M) was proposed in ref. [27], although we do not use that here.

where $n_{\rm F}$ is the Fermi-Dirac distribution, $\mathbb{P}$ stands for the Cauchy principal value and g and $\boldsymbol{f}$ are Green's functions satisfying

$$(\hat{H} + i0^+)g(\boldsymbol{b}) \;=\; \delta^{(2)}(\boldsymbol{b})\,, \quad (\hat{H} + i0^+)\boldsymbol{f}(\boldsymbol{b}) \;=\; -\nabla_\perp \delta^{(2)}(\boldsymbol{b})\,. \tag{13}$$

The operator $\hat{H}$ acts in the transverse plane,

$$\hat{H} = \frac{\omega(M_{\rm eff}^2 - \nabla_\perp^2)}{2p(\omega - p)} + ig^2 C_{\rm F} T \int \frac{{\rm d}^2\boldsymbol{q}}{(2\pi)^2}(1 - e^{i\boldsymbol{q}\cdot\boldsymbol{b}})\Big(\frac{1}{q^2} - \frac{1}{q^2 + m_D^2}\Big)\,, \tag{14}$$

where $M_{\rm eff}^2 \equiv m_\infty^2 - \frac{p(\omega-p)}{\omega^2}M^2$.

In order to combine the LPM and NLO results, we also need to naively expand the LPM results up to $O(g^2)$ and remove double counting *à la* eq. (4). At zeroth order in g, the expression becomes

$$\rho_{\rm V}\big|_{\rm LPM}^{(g^0)} \;=\; \frac{N_{\rm c} M^2}{4\pi}\Big\{ \sum_{\nu=\pm\mu} \frac{T}{\omega} \ln\Big[\frac{1 + e^{(\nu-\omega)/T}}{1 + e^{\nu/T}}\Big] + \Theta(K^2)\Big\}\,, \tag{15}$$

which matches (3) for $\omega \simeq k$. The corrections of $O(g^2)$ are proportional to m_∞^2 . As in the $\mu = 0$ case [9], the spectral function $\rho_{\rm V}$ contains a log-divergence plus a finite part:

$$\rho_{\rm V}\big|_{\rm LPM}^{(g^2)} \;=\; \frac{N_{\rm c} m_\infty^2}{4\pi}\Big\{\Big[1 - n_{\rm F}(\omega - \mu) - n_{\rm F}(\omega + \mu)\Big]\Big(\ln\Big|\frac{m_\infty^2}{M^2}\Big| - 1\Big) + \mathcal{F}(\omega)\Big\} \tag{16}$$

where

$$\begin{aligned}\mathcal{F}(\omega) \;\equiv\; & \Big[\Theta(K^2)\int_0^\omega {\rm d}p - \Theta(-K^2)\Big(\int_{-\infty}^0 + \int_\omega^\infty\Big){\rm d}p\Big]\Big\{2\,\frac{1 - n_{\rm F}(p-\mu) - n_{\rm F}(\omega - p + \mu)}{\omega} \\ & - \frac{n_{\rm F}(-\mu) + n_{\rm F}(\omega+\mu) - n_{\rm F}(p-\mu) - n_{\rm F}(\omega - p + \mu)}{p} \\ & - \frac{n_{\rm F}(\omega-\mu) + n_{\rm F}(\mu) - n_{\rm F}(p-\mu) - n_{\rm F}(\omega - p + \mu)}{\omega - p}\Big\}\,.\end{aligned} \tag{17}$$

The log-divergence in (16) exactly matches that from $\rho_{\rm V}|_{\rm NLO}^{(g^2)}$, and the full resummed expression is finite and continuous across the light cone. This is illustrated in fig. 3 at $\mu = 2T$ for fixed coupling $\alpha_s = 0.3$. (We have also verified this cancellation analytically.) Although not visible from fig. 3, the presence of μ enhances the LPM rate due to a larger m_∞ which sets the overall scale. This enhancement counteracts the suppressing effect of μ in the 1-loop spectral function (3).

6 Outlook

The emission rate of thermal photons and dileptons can be derived from the same underlying spectral function $\rho_{\rm V}$, which encodes all orders in α_s. After a long history of computing the perturbative corrections in various limits, there is now sufficient information to interpolate between these regimes as suggested by ref. [5]. The utility of having a model of the spectral function for all ω is that it allows for comparison with lattice data at non-zero momentum. One may also use the pertubative result to create 'mock data' for testing methods of reconstructing $\rho_{\rm V}$ from (6), e.g. the Backus-Gilbert method.

A natural next step is to implement the thermal rates calculated from (4) in hydrodynamic simulations of relativistic heavy ion collisions [28]. (Early studies in this direction can be

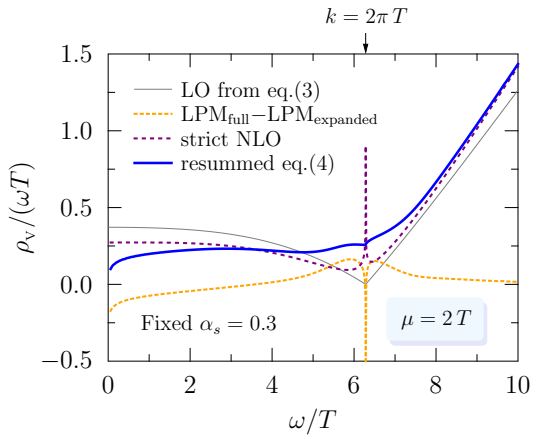

Figure 3. The vector channel spectral function, plotted as a function of ω for $k = 2\pi T$ and with $\alpha_s = 0.3$. This illustrates both the strict loop expansion from sec. 4 (dashed) and the relevant LPM part from sec. 5 (dotted) where the log-divergence for $\omega \approx k$ from (16) is evident. Crucially, the prescription of eq. (4) gives a result (solid) that is both finite and continuous at the light cone. (For comparison, the free result is also shown.)

found in ref. [29].) For example, the fully differential dilepton rate, with $\alpha_{\rm em} = e^2/(4\pi)$ and for $n_f = 3$ reads

$$\frac{\mathrm{d}\Gamma_{\ell\bar{\ell}}(\omega,k)}{\mathrm{d}\omega\,\mathrm{d}^3\boldsymbol{k}} = 2\frac{\alpha_{\rm em}^2 n_{\rm B}(\omega)}{9\pi^3 M^2}\,B\!\left(\frac{m_\ell^2}{M^2}\right)\rho_{\rm V}(\omega,k)\,, \tag{18}$$

where $n_{\rm B}$ is the Bose distribution function and the phase space factor is $B(x) \equiv (1+2x)\Theta(1-4x)\sqrt{1-4x}$. The M-distribution that follows is shown in fig. 4 for several temperatures (at zero net baryon density) which are expected to be probed in central collisions at the LHC and RHIC facilities. Since $\mathrm{d}\Gamma_{\ell\bar{\ell}}$ represents the rate per unit volume, the result shown still needs to be convoluted with the spacetime evolution of the fireball. This task is left for future work

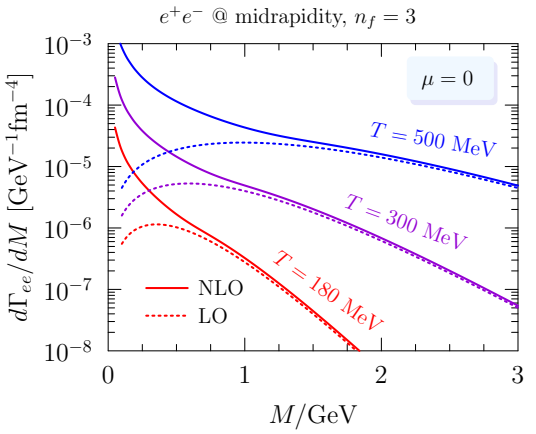

Figure 4. Invariant mass distribution of the differential rate to product an e^+e^- pair, $\mathrm{d}\Gamma_{ee} \equiv \mathrm{d}N/\mathrm{d}^4X$, computed from eq. (18) after converting to hyperbolic coordinates and integrating over the azimuthal angle and $k_\perp$ at midrapidity. We show the resummed NLO result from (4) (solid) and the LO result from (3) (dotted), at the temperatures $T = \{180, 300, 500\}$ MeV. The running of α_s has been implemented as described in ref. [9].

Acknowledgements

Let me express my gratitude to D. Bala, J. Churchill, C. Gale, J. Ghiglieri, S. Jeon, O. Kaczmarek and M. Laine for many helpful discussions and their ongoing collaboration on several aspects of this topic. Furthermore, I thank J. Ghiglieri for providing the LPM$^{\rm NLO}$ data from ref. [24], and D. Bala and O. Kaczmarek for providing the quenched lattice data shown in

fig. 2. I am also grateful to T. Gorda, K. Seppänen and R. Paatelainen for their assistance in cross-checking these results in the HTL limit [26]. This work was supported by the U.S. Department of Energy (DOE) under grant No. DE-FG02-00ER41132.

References

[1] L.D. McLerran, T. Toimela, Phys. Rev. D **31**, 545 (1985)
[2] H.A. Weldon, Phys. Rev. D **42**, 2384 (1990)
[3] C. Gale, J.I. Kapusta, Nucl. Phys. B **357**, 65 (1991)
[4] H. Gervais, S. Jeon, Phys. Rev. C **86**, 034904 (2012), 1206.6086
[5] I. Ghisoiu, M. Laine, JHEP **10**, 083 (2014), 1407.7955
[6] M. Laine, A. Vuorinen, *Basics of Thermal Field Theory*, Vol. 925 (Springer, 2016), 1701.01554
[7] H.B. Meyer, M. Cè, T. Harris, A. Toniato, C. Török, PoS **LATTICE2021**, 269 (2022), 2112.00450
[8] A. Dumitru, D.H. Rischke, T. Schönfeld, L. Winckelmann, H. Stöcker, W. Greiner, Phys. Rev. Lett. **70**, 2860 (1993)
[9] G. Jackson, M. Laine, JHEP **11**, 144 (2019), 1910.09567
[10] M. Laine, JHEP **05**, 083 (2013), 1304.0202
[11] E. Braaten, R.D. Pisarski, T.C. Yuan, Phys. Rev. Lett. **64**, 2242 (1990)
[12] J.I. Kapusta, P. Lichard, D. Seibert, Phys. Rev. D **44**, 2774 (1991), [Erratum: Phys.Rev.D 47, 4171 (1993)]
[13] R. Baier, H. Nakkagawa, A. Niegawa, K. Redlich, Z. Phys. C **53**, 433 (1992)
[14] P. Aurenche, F. Gelis, H. Zaraket, JHEP **07**, 063 (2002), hep-ph/0204145
[15] P. Aurenche, F. Gelis, G.D. Moore, H. Zaraket, JHEP **12**, 006 (2002), hep-ph/0211036
[16] P.B. Arnold, G.D. Moore, L.G. Yaffe, JHEP **11**, 057 (2001), hep-ph/0109064
[17] P.B. Arnold, G.D. Moore, L.G. Yaffe, JHEP **12**, 009 (2001), hep-ph/0111107
[18] G. Jackson, M. Laine, JHEP **09**, 125 (2021), 2107.07132
[19] G. Jackson, Phys. Rev. D **100**, 116019 (2019), 1910.07552
[20] H.B. Meyer, Eur. Phys. J. A **47**, 86 (2011), 1104.3708
[21] G. Aarts, C. Allton, J. Foley, S. Hands, S. Kim, Phys. Rev. Lett. **99**, 022002 (2007), hep-lat/0703008
[22] B.B. Brandt, A. Francis, T. Harris, H.B. Meyer, A. Steinberg, EPJ Web Conf. **175**, 07044 (2018), 1710.07050
[23] J. Ghiglieri, O. Kaczmarek, M. Laine, F. Meyer, Phys. Rev. D **94**, 016005 (2016), 1604.07544
[24] J. Ghiglieri, G.D. Moore, JHEP **12**, 029 (2014), 1410.4203
[25] G. Jackson, Ph.D. thesis, U. Bern, AEC (2020)
[26] T. Gorda, A. Kurkela, J. Österman, R. Paatelainen, S. Säppi, P. Schicho, K. Seppänen, A. Vuorinen (2022), 2204.11279
[27] J. Ghiglieri, M. Laine, JHEP **01**, 173 (2022), 2110.07149
[28] J. Churchill, Ph.D. thesis, McGill U. (2022)
[29] Y. Burnier, C. Gastaldi, Phys. Rev. C **93**, 044902 (2016), 1508.06978